Stability of Binary Solitons in Optical Fibers with Cubic-Quintic Cross-Phase Modulation

S. Das[a,b] and G.A. Sekh[a,*]

[a] *Department of Physics, Kazi Nazrul University, Asansol-713340, India*
[b] *Department of Physics, Government General Degree College, Chapra Shikra, Nadia-741123, India*

Received: 28.02.2022 & Accepted: 23.10.2022

Doi: 10.12693/APhysPolA.142.450 *e-mail: golamali.sekh@knu.ac.in

We consider the propagation of nonlinear coupled pulses in an optical fiber with cubic-quintic self-and cross-phase modulation. We model the system by extended Manakov equations incorporating higher-order cross-coupling terms. We find that the pulse gets a certain minimum width for stable propagation in the medium. However, the pulse width reduces in the presence of higher-order cross-coupling terms. We make use of the Vakhitov–Kolokolov criterion and examine whether the pulse is linearly stable for different values of the pulse power. We also simulate the dynamics of a coupled soliton by a purely numerical routine.

topics: optical solitons, manakov model, variational approach, Vakhitov–Kolokolov criterion

1. Introduction

Soliton is a nonlinear wave that emerges from the interplay between non-linear and dispersion effects. During propagation, the shape and velocity of the solitons remain unaltered. Interestingly, all properties of solitons, except phase, remain invariant after collisions. However, the propagation of solitons in a particular medium is largely affected by the variation of the frequency and intensity of the pulse [1, 2]. More specifically, a high-frequency solitary wave (short pulse) enhances the dispersive effects, while its intensity affects the non-linearity of the optical medium. In the optical medium, the primary dispersive and nonlinear effects are respectively the group velocity dispersion (GVD) and the Kerr effects, which are responsible for the formation of the fundamental soliton. The properties of the shorter and highly intense pulse, however, are affected by the presence of non-Kerr effects like quintic non-linearity, stimulated Raman scattering, self-steepening, two-photon absorption, third-order dispersion etc. Most of the non-Kerr effects start to play if the optical pulse is very short (< 100 fs). Mathematically, such pulses can be described by the generalized Kundu–Eckhaus equation [3, 4]. There exists several studies based on the model [5, 6]. Recently, on the basis of the model, the existence of dipole soliton was predicted under some parametric conditions [7]. New types of solitary waves with the combined properties of a dark and bright soliton have been reported in [8].

For a pulse having a width greater than 100 fs and of moderate intensity, the dominant non-Kerr effect is quintic nonlinearity [3]. In this case, the displacement vector of the dielectric medium becomes the square function of the electric-field amplitudes, and the refractive index of the medium, if expressed in terms of the intensity of the medium, can be written as $n = n_0 + n_2 I + n_4 I^2$, where n_0 is the linear refractive index, and n_2 and n_4 are the refractive indexes of cubic and quintic nonlinearities, respectively. Studies on cubic-quintic nonlinear media have renewed considerable interest due to the technological development for inducing artificial higher order-nonlinearities in optical materials like semiconductor doped glasses, chalcogenide glasses, organic polymers [9–12] and possible applications. The system supports interesting phenomenon which include pulse compression [13], Town's solitons [14] and cicular soliton [15].

In addition to the scalar soliton, a single-mode birefringent fiber or multi-mode fiber can support a pair of solitons such as bright–bright, dark–dark, which are coupled through cross-phase modulation (XPM) [16, 17]. Recently, incoherently coupled dark–bright (DB) vector solitons have been observed experimentally. It was found that, unlike the scalar soliton, the dark–bright vector solitons are formed in single-mode fibers for both normal and anomalous group velocity dispersion (GVD) [18]. All studies are based either on the Manakov model or the Helmholtz–Manakov model, where XPM is cubic. Since at a moderate intensity the quintic nonlinearity comes into play, it can induce intermodal interaction between pulses through quintic XPM [3, 19, 20].

Our objective in this work is to envisage a theoretical study on the coupled bright solitons (BB-type) considering cubic and quintic XPM, in order to see what is the effect of cross-phase modulation (XPM) due to quintic nonlinearity on the formation of BB-type solitons. We work with the extended Manakov model within the framework of variational approach. Based on a similar model, Qi et al. [20] predicted the generation of soliton solutions due the Darboux transformation and symbolic computations [20]. Recently, Yan et al. [19] found the existence of a bright–dark rogue wave and a breather wave using Darboux dressing transformation and asymptotic expansion.

In Sect. 2 we introduce a variational approach to deal with the problem of bright–bright solitons supported by the system [3]. We find the effective potential for the pulse width and find the minimum value of the pulse width. In Sect. 3, we find the linear spectrum corresponding to each component of the soliton and present the linear stability analysis. We check the dynamical stability by directly simulating the time evolution of solitons. We restore the physics unit from the normalized units and compare it with the experimental result. We outline the main result of the paper in Sect. 4.

2. Formulation of the problem within variational framework

Propagation of a single pulse in cubic–cubic quintic nonlinear media is described by the following nonlinear Schrödinger equation [21–25]

$$\mathrm{i}\, u_x = C\, u_{tt} + 2\big(\alpha\, |u|^2 + \gamma\, |u|^4\big) u. \tag{1}$$

Here, α and γ are the coefficients of the third- and fifth-order nonlinear coefficients, respectively. The numerical values of the parameters can be positive or negative depending on the properties of the medium and the pulse frequency. For an ultrashort optical pulse, there can be two interesting effects, namely nonlinear dispersion/self-steepening and Raman scattering resulting in velocity change and frequency shift of the pulse [24]. However, these effects are negligible for pulses with a width greater than 100 fs at moderate intensity. If we allow two such pulses to propagate simultaneously in a nonlinear medium, then the coupling comes into play due to the inter-pulse interaction. Coupled vector soliton can be treated as incoherently coupled two orthogonal linearly polarized light waves in a birefringent single-mode fiber [26], in which the modal dispersion is the lowest. Mathematically, the simultaneous propagation of two pulses can be described by the extended Manakov model [20]

$$\mathrm{i}\, u_{jx} = C_j u_{jtt} + 2\big(\alpha_j |u_j|^2 + \gamma_j |u_j|^4\big) u_j + \beta_j |u_{3-j}|^2 u_j + \delta_j |u_{3-j}|^4 u_j + 2\delta_{3-j} |u_j|^2 |u_{3-j}|^2 u_j, \tag{2}$$

where $u_j(t,x)$ $(j=1,2)$ represents the complex amplitudes or envelopes of the two pulses having orthogonal polarizations; C_j represents the group velocity dispersion (GVD) coefficient. The parameters α_j and γ_j stand for the strengths of self-phase modulations arising due to cubic- and quintic- nonlinearity. The factor β represents the strength of cubic cross-phase modulation XPM, whereas δ_j stands for the quintic XPM. One can check that (2) is obtained from (1) by substituting $u = \sum_{j=1}^{2} a_j\, u_j$ and applying orthogonality condition or by substituting the same in the Kundu–Eckhaus equation in the negligible nonlinear dispersion limit [3, 19, 20]. Note that (2) can also describe coupled pulse propagation in a multimode fiber (MMF). The modal dispersion in that case is large. However, the inter-modal dispersion can be optimized by choosing the appropriate fiber. For example, in a graded index fiber where the refractive index (r.i.) varies in a parabolic pattern (called a parabolic index fiber), inter-modal dispersion is minimum. A step index fiber is one where r.i. faces sharp changes and can act as a multimode fiber with negligible inter-modal dispersion.

The action functional for (2) can be expressed as

$$\mathcal{I} = \int \mathrm{d}x \int \mathrm{d}t\, \mathcal{L}\Big(u_1, u_1^*, u_2, u_2^*, u_{1x}, u_{1x}^*, u_{2x}, u_{2x}^*, u_{1t}, u_{1t}^*, u_{2t}, u_{2t}^*\Big) \tag{3}$$

where

$$\mathcal{L} = \sum_{j=1}^{2} \left[\frac{\mathrm{i}}{2}\left(u_{jx}u_j^* - u_{jx}^* u_j\right) + C_j\, |u_{jt}|^2 - \alpha_j |u_j|^4 - \frac{2}{3}\gamma_j |u_j|^6 - \delta_j |u_{3-j}|^4 |u_j|^2\right] - \beta |u_1|^2 |u_2|^2. \tag{4}$$

The cubic-quintic nonlinear Schrödinger equation supports both bright solitons [27, 28]. Clearly, (1) follows the action principle in (4). Assuming a weak XPM, we adopted a Gaussian-shaped function

$$u_j(x,t) = A_j(x) \exp\left(-\frac{t^2}{2a_j(x)^2} + \mathrm{i} b_j(x) t^2 + \mathrm{i}\phi_j\right) \tag{5}$$

as trial solutions of the coupled system. Here, $A_j(0)$, $a_j(0)$, and $b_j(0)$ represent the amplitude, width and frequency chirp of the pulses at $x=0$, respectively, while the complex amplitude $A_j(x)$, the pulse width $a_j(x)$, the frequency chirp $b_j(x)$ will all vary with the propagation distance. Understandably, (3) describes bright–bright-type (BB-type) solution [29].

Inserting (3) in (2) and integrating over x from $-\infty$ to $+\infty$, we get $\langle \mathcal{L} \rangle$. From the vanishing condition of the variational derivative of $\delta \langle \mathcal{L} \rangle / \delta X_j = 0$ for $X_j(x) \equiv A_j(x), a_j(x), b_j(x)$ and ϕ_j, one can find equations for variational parameters. A proper combination of these equations lead us to write the following equations for the parameters

$$a_j |A_j|^2 = \frac{E_j}{\sqrt{\pi}} = P_j, \tag{6}$$

$$a_j^2 \frac{\mathrm{d}b_j}{\mathrm{d}x} = -\frac{C_j}{a_j^2} + 4C_j a_j^2 b_j^2 + \frac{\sqrt{2}\,\alpha_j P_j}{a_j} + \frac{4}{3\sqrt{3}}\frac{\gamma_j P_j^2}{a_j^2} + \frac{2\beta\, a_j^2 P_{3-j}}{\left(a_j^2 + a_{3-j}^2\right)^{3/2}} + T_j, \tag{7}$$

with

$$T_j = 8P_j P_{3-j} C_j\, \frac{(a_j^2 + a_{3-j}^2)\delta_{3-j}}{a_j^2 (a_j^2 + 2a_{3-j}^2)^{3/2}} + 8P_{3-j}^2 C_j\, \frac{a_j \delta_j}{a_{3-j}(a_j^2 + 2a_{3-j}^2)^{3/2}} \tag{8}$$

and

$$b_j = -\frac{1}{4} C_j^{-1} a_j^{-1}\, \frac{\mathrm{d}a_j}{\mathrm{d}x}. \tag{9}$$

In (6), P_j stands for the initial energy of the optical pulses. Mathematically, it represents the norm $P_j = \int_{-\infty}^{+\infty} \mathrm{d}t\, |u_j|^2$ of the system. Thus, (6) implies the non-dissipative pulse propagation. Combining (7) with the frequency chirp evolution (8), we get the evolution of the pulse width, i.e,

$$\frac{\mathrm{d}^2 a_j}{\mathrm{d}x^2} = \frac{4C_j^2}{a_j^3} - \frac{2\sqrt{2}\,\alpha_j C_j P_j}{a_j^2} - \frac{16}{3\sqrt{3}}\,\frac{\gamma_j C_j P_j^2}{a_j^3} - \frac{8\beta\, C_j a_j P_{3-j}}{\left(a_j^2 + a_{3-j}^2\right)^{3/2}} + T_j. \tag{10}$$

The effective potential $V(a_1, a_2)$ for the coupled pulse can be obtained as

$$C_j^{-1} P_j \frac{\mathrm{d}^2 a_j}{\mathrm{d}x^2} = -\frac{\partial V_j(a_1, a_2)}{\partial a_j}, \tag{11}$$

where effective potential for each component V_j is given by

$$V_j = V_j^{SP} + V_j^{PX2} + V_j^{PX3} \tag{12}$$

with

$$V_j^{SP} = \frac{2P_j C_j}{a_j^2} - \frac{2\sqrt{2}\,\alpha_j P_j^2}{a_j} - \frac{8}{3\sqrt{3}}\,\frac{\gamma_j P_j^3}{a_j^2}, \tag{13}$$

$$V_j^{XP2} = -\frac{8\beta\, P_j P_{3-j}}{\sqrt{a_1^2 + a_2^2}}, \tag{14}$$

$$V_j^{XP3} = -\frac{4P_j^2 P_{3-j}\delta_{3-j}}{a_j\sqrt{a_j^2 + 2a_{3-j}^2}} - \frac{4P_j P_{3-j}^2 \delta_j}{a_{j-3}\sqrt{2a_j^2 + a_{3-j}^2}}. \tag{15}$$

Clearly, the effective potential consists of three terms whose origins are quite distinct. The first term comes from self-phase modulation (cubic and quintic) and second order group velocity dispersion. The second and third terms stand for cubic- and quintic XPM.

3. Dynamical interplay and linear stability analysis of BB-type solitons

In order to understand the dynamical inter-play among different types of nonlinearity and dispersive effect in the formation of BB-type solitons, we consider the effective potential given in (12). For simplicity of presentation, we first consider that the two orthogonal components have equal widths, which implies that the ratio P_j/A_j^2 is the same for both pulses. In this situation, two cases may arise, namely (i) $P_1 = P_2$ and (ii) $P_1 \neq P_2$. For a case (i), we plot in Fig. 1, the effective potential $\tilde{V}_j (= V_j/P_j)$ as a function of the pulse widths a_j. Three different potentials are shown for the quintic XPM δ. Here, we take $\delta_1 = \delta_2 = \delta$. Figure 1 clearly demonstrates the fact that for $\delta \neq 0$, the soliton's width squeezes to form a shorter pulse. One can check that the pulse width corresponding to the minima of the curve for $\delta = 0$ and $\delta \neq 0$ squeezes up to 60%. We further infer from the results in Fig. 1 that there must be some threshold value of a_j above which the GVD dominates, and thus the pulse becomes dispersive.

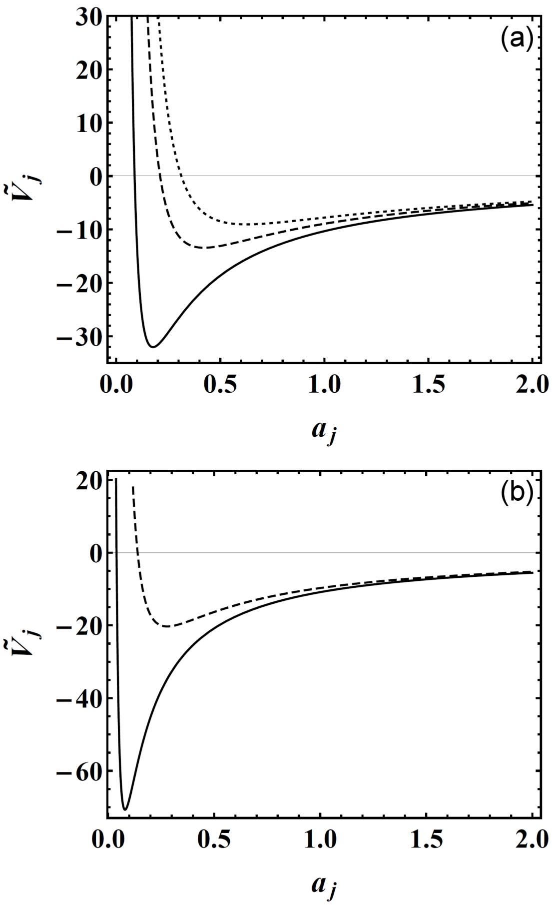

Fig. 1. (a) Formation of a short pulse in the presence of quintic XPM. The dotted, dashed, and solid curves give the effective potential for $\delta = 0.0$, 0.1, and 0.55, respectively, when $P_1 = P_2 = 1.0$. Other parameters are fixed as: $C_j = 1$, $\alpha = 2$, $\beta = 2$, $\gamma_1 = -1$, and $\gamma_2 = -1$. (b) The dashed ($j = 1$) and solid ($j = 2$) curves give the effective potential for $\delta = 0.55$ when $P_1 = 1.1$ and $P_2 = 0.9$. Other parameters are fixed as: $C_j = 1$, $\alpha = 2$, $\beta = 2$, $\gamma_1 = -1$, and $\gamma_2 = -1$.

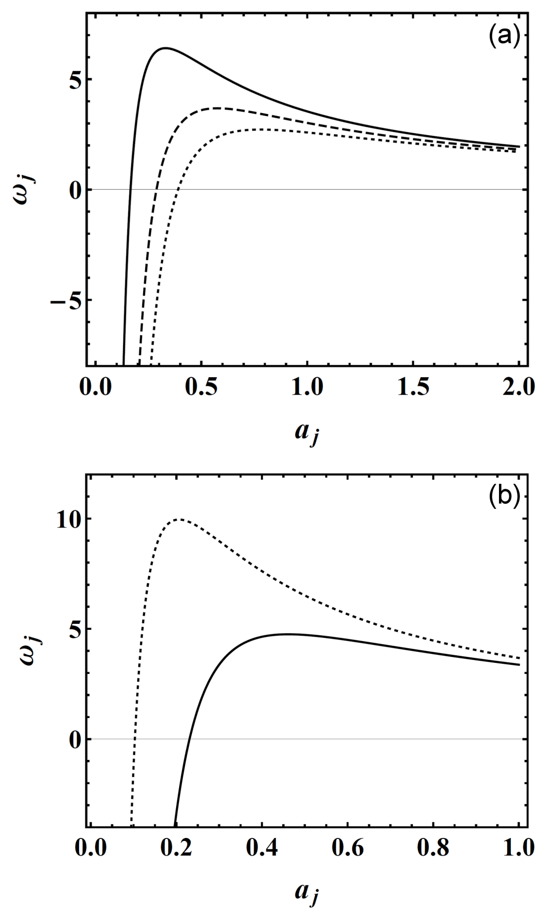

Fig. 2. Stability of a short pulse in the presence of quintic XPM. (a) The dotted, dashed, and solid curves give the variation of spectral frequencies with the pulse width of 0, 0.25, and 0.55, respectively, when $P_1 = P_2 = 1.0$. (b) The dotted ($j = 1$), solid ($j = 2$) curves give the spectral frequencies for $\delta = 0.55$ when $P_1 = 1.1$ and $P_2 = 0.9$. Other parameters are fixed as: $C_j = 1$, $\alpha = 2$, $\beta = 2$, $\gamma_1 = -1$, and $\gamma_2 = -1$.

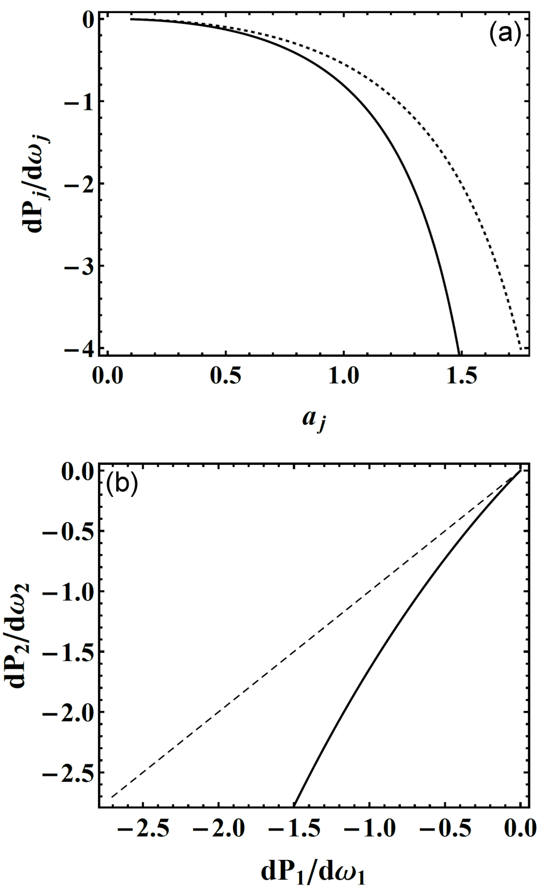

Fig. 3. Stability of a short pulse in the presence of quintic XPM. (a) The dotted ($j = 1$) and solid ($j = 2$) curves give the spectral frequencies for $\delta = 0.55$ when $P_1 = 1.1$ and $P_2 = 0.9$. (b) Gradient of optical power with spectral frequency for different values of pulse width. Other parameters are fixed as: $C_j = 1$, $\alpha = 2$, $\beta = 2$, $\gamma_1 = -1$, $\gamma_2 = -1$, and $\delta = 0.55$.

If the initial energies of the pulses are taken slightly differently, the system supports shorter pulses in the presence of quintic cross coupling terms. Figure 1 clearly shows that the minimum occurs at $a = 0.08$ for $P_2 = 0.9$, while at $a = 0.177$ for $P_1 = 1.1$. This arises due to the fact that the dispersive effect dominates over the nonlinear effect for $P_1 > P_2$.

In order to check the linear stability of the coupled stationary solitary waves, we make use of the *generalised Vakhitov–Kolokolov criterion* [30–32]. To do this, we replace $u_1(t,x) \to u_1(t)\mathrm{e}^{-\mathrm{i}\omega_1 x}$ and $u_2(t,x) \to u_2(t)\mathrm{e}^{-\mathrm{i}\omega_2 x}$ in (1) with the ω_j frequency of the linear spectrum, and write

$$\omega_1 = \frac{C_1}{2a_1^2} - \frac{2\gamma_1 P_1^2}{\sqrt{3}a_1^2} - \frac{\sqrt{2}\alpha_1 P_1}{a_1} - \frac{\delta_1 P_2^2}{a_2\sqrt{a_2^2+2a_1^2}} - \frac{\beta P_2}{\sqrt{a_1^2+a_2^2}} - \frac{2P_1P_2\delta_2}{a_1\sqrt{2a_2^2+a_1^2}} \tag{16}$$

and

$$\omega_2 = \frac{C_2}{2a_2^2} - \frac{2\gamma_2 P_2^2}{\sqrt{3}a_2^2} - \frac{\sqrt{2}\alpha_2 P_2}{a_1} - \frac{\delta_2 P_1^2}{a_1\sqrt{a_1^2+2a_2^2}} - \frac{\beta P_1}{\sqrt{a_2^2+a_1^2}} - \frac{2P_1P_2\delta_1}{a_2\sqrt{2a_1^2+a_2^2}} \tag{17}$$

for the first and second components, respectively. Here, we deal with the case where the total pulse energy is fixed such that $P_0 = P_1 + P_2$. In Fig. 2 we display the variation of ω_j for equal energetic pulses for different values of quintic XPM. Figure 2 clearly shows that the changes of the sign of gradient of ω_j take place around $a_j \approx 0.17$, which is consistent with the effective potential model (the minimum of solid curve in Fig. 1). Interestingly, if the energies of the two pulses differ slightly (Fig. 2b), we can see that the gradient of ω_j for a lower energetic pulse changes its sign at smaller value of a_j. Therefore, the coupled pulse in the presence of the quintic XPM is also linearly stable for both $P_1 = P_2$ and $P_1 \neq P_2$.

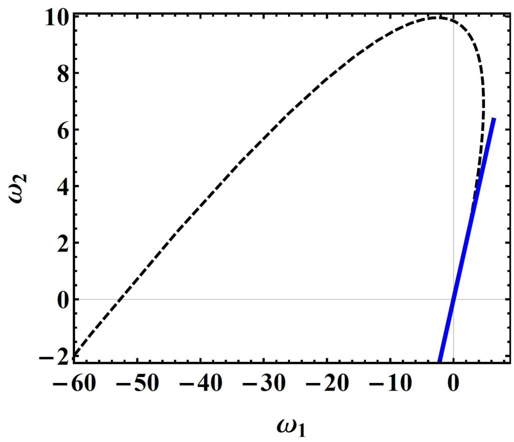

Fig. 4. Stability of a short pulse in the presence of quintic XPM. It shows ω_1 versus ω_2 for $P_1 = P_2 = 1.0$ (blue) and $P_1 = 1.1, P_2 = 0.9$ (black dashed). Other parameters are fixed as: $C_j = 1$, $\alpha = 2$, $\beta = 2$, $\gamma_1 = -1$, $\gamma_2 = -1$ and $\delta = 0.55$.

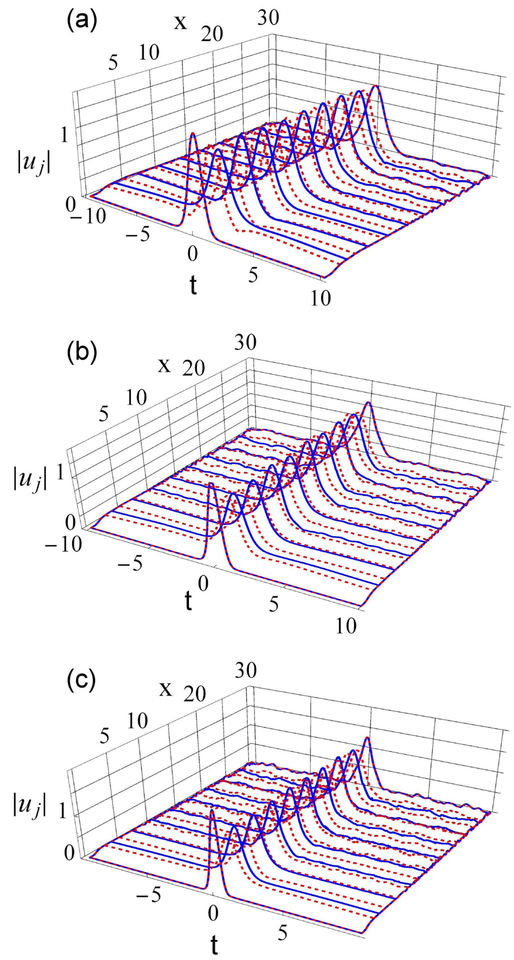

Fig. 5. Evolution of a short pulse in the presence of cubic-quintic XPM. (a) The solid blue ($j = 1$) and dashed red ($j = 2$) curves give density for $\delta = 0.0$, $a_1 = a_2 = 0.55$ when $P_1 = P_2 = 1$. (b) Similar to panel (a) but for $\delta = 0.25$ and $a_1 = a_2 = 0.41$. (c) Similar to panel (a) but for $\delta = 0.55$ and $a_1 = a_2 = 0.3$.

The changes of P_j with respect to the spectral frequency ω_j play an important role in the examination of the stability of solitary waves. For example, if $\frac{\mathrm{d}P_j}{\mathrm{d}\omega_j} < 0$, then the solitary wave is stable, otherwise it is unstable. This is the so-called Vakhitov–Kolokolov stability criterion. In Fig. 3a, it is clear that BB-type solitons are linearly stable since $\frac{\mathrm{d}P_j}{\mathrm{d}\omega_j} < 0$ is negative in both cases. The values of $\frac{\mathrm{d}P_1}{\mathrm{d}\omega_1}$ and $\frac{\mathrm{d}P_2}{\mathrm{d}\omega_2}$ are equal for $P_1 = P_2$, but they are unequal for $P_1 \neq P_2$ (Fig. 3b). It is worth to note that the sign of $\frac{\mathrm{d}P_j}{\mathrm{d}\omega_j} < 0$ depends on the relative values of ω_1 and ω_2. Therefore, we need to find the appropriate points in the $\omega_1 - \omega_2$ plane for the stable coupled pulse propagation.

In view of the above, we plot in Fig. 4 the variation of the relative values of ω_1 and ω_2 for different pulse widths. Here, the solid blue and black dashed curves correspond to cases of $P_1 = P_2$ and $P_1 \neq P_2$, respectively. In the $\omega_1 - \omega_2$ plane, the spectral frequency for BB-type solitons is positive only in the first quadrant and thus it can give stable solitary waves in the presence of cubic-quintic cross-phase modulation.

We calculate numerically the density profile of a linearly stable BB-type coupled pulse at different time for the initial condition $u_j(t, 0) = A_j \exp[-t^2/(2a_j^2)]$ and the boundary condition $u_j(-20, x) = u_j(+20, x)$. The variation of density profile in Fig. 5 clearly indicates that a solitary solution remains stable and the effects of XPM reduce the pulse widths.

In the above, we present the result considering all parameters in normalized units. Sometimes it is helpful to check feasibility by expressing the parameters in physical units. Writing (1), we have scaled $u_j = (\eta A_{\mathrm{eff}})^{1/2} u'_j$ such that $|u_j|^2$ becomes the wave power [33]. The quantity A_{eff} is the effective mode area of fiber associated with cubic nonlinearity. In this work, the coefficient of cubic nonlinear terms α and β are scaled by $\tilde{\alpha} = |\frac{2\pi n_2}{\lambda A_{\mathrm{eff}}}|$ and qunitic nonlinear terms γ and δ by $\tilde{\gamma} = |\frac{2\pi n_4}{\lambda A_{\mathrm{eff}\,1}}|$. Here $A_{\mathrm{eff}\,1} \approx \frac{3}{4} A_{\mathrm{eff}}$ [34]. When measuring z and τ we use the units of dispersive length (L_D) and initial pulse width (T_0), respectively [35]. Here, $L_D = T_0^2/|2C_j|$. A typical value of A_{eff} varies from 25 to 126 μm^2. For the propagation of Gaussian shaped pulse at a wavelength 1.55 μm and $C_j = 1$ ps^2/(K m) in the normal-GVD fiber for $n_2 = 2.7 \times 10^{-13}$ cm^2/W, $n_2 = -7.8 \times 10^{-23}$ cm^2/W and $A_{\mathrm{eff}} = 40$ μm^2, one can calculate $\tilde{\alpha} = 2.736 \times 10^3$ W^{-1} K^{-1} m^{-1} and $\tilde{\gamma} = 2.63$ W^{-2} K^{-1} m^{-1} [18, 36]. For the initial pulse $u_j(0, t) = (\frac{E_j}{\sqrt{\pi} a_j})^{1/2} \mathrm{e}^{-t^2/(2a_j^2)}$, the pulse width for stable propagation is $w_s = a_j T_0$. In standard telecommunication, L_D is approximately 5 Km for the initial pulse power $\simeq$ 200 mW, and thus

$T_0 \approx 3.3$ ps. In the present variational calculation, we get $a_j \sim 0.5$ for $\delta = 0$ while $a_j \sim 0.3$ for $\delta = 0.55$. Therefore, we see that the coupled optical pulse of the full width at half maximum (FWHM) $\lesssim 1$ ps can be supported by a nonlinear media with cubic-quintic self- and cross-phase modulations.

4. Conclusion

In this work, we have considered coupled optical pulses of moderate intensity (frequency > 100 fs) with special attention to cubic-quintic self-phase and cross-phase modulations. We formulate the problem within the framework of the variational approach and find the effective potential for the pulse width. It is found that the effective potential attains the minimum value for a particular value of pulse width. The value of the optimal pulse width changes with the strength of self- and cross-phase modulation arising from the cubic–quintic interaction. We find that the quintic cross-phase can play a significant role in pulse compression. We remark that the squeezing will be limited by nonlinear dissipation and the Kundu–Eckhaus model should be taken into account.

We made a linear stability analysis of the coupled pulses by the use of the Vakhitov–Kolokolov criterion and found that the pulse supported by the system due to higher-order cross-coupling is shorter and linearly stable. We find the region of stability of the coupled pulses and see that it depends on the relative energy value of the two pulses.

We simulate the dynamics of the system using using the split-step Fourier method for pulses with parameters obtained from optimization procedure followed by Vakhitov–Kolokolov criterion. More specifically, we study the time evolution of the pulse for different values of the XPM strengths. It is found that the pulses are dynamically stable. We also check the feasibility of the results using experimental parameters.

Acknowledgments

One of the authors (GS) would like to acknowledge the funding from the "Science and Engineering Research Board (SERB), Govt.of India" through Grant No. CRG/2019/000737.

References

[1] G.P. Agrawal, *Nonlinear Fiber Optics*, 5th Ed., Academic Press, 2012.

[2] L.F. Mollenauer, J.P. Gordon, *Solitons in Optical Fibers: Fundamentals and Applications*, 1st Ed., Academic Press, 2006.

[3] R. Radhakrishnan, A. Kundu, M. Lakshmanan, *Phys. Rev. E* **60**, 3314 (1999).

[4] A. Kundu, *J. Math. Phys.* **25**, 3433 (1984).

[5] S.L. Palacios, A. Guinea, J.M. Fernandez-Diaz, R.D. Crespo, *Phys. Rev. E* **60**, R45(R) (1999).

[6] M. Gedalin, T.C. Scott, Y.B. Band, *Phys. Rev. Lett.* **78**, 448 (1997).

[7] A. Choudhuri, K. Porsezian, *Opt. Commun.* **285**, 364 (2012).

[8] Z. Li, L. Li, H. Tian, G. Zhou, *Phys. Rev. Lett.* **84**, 4096 (2000).

[9] J.L. Coutaz, M. Kull, *J. Opt. Soc. Am. B* **8**, 95 (1991).

[10] P. Roussignol, D. Ricard, J. Lukasik, C. Flytzanis, *J. Opt. Soc. Am. B* **4**, 5 (1987).

[11] L.H. Acioli, A.S.L. Gomes, J.R. Rios Leite, *Appl. Phys. Lett.* **53**, 1788 (1988).

[12] J. Arabat, J. Etchepare, *J. Opt. Soc. Am. B* **10**, 2377 (1993).

[13] K. Senthilnathan Q. Li, K. Nakkeeran, P.K.A. Wai, *Phys. Rev. A* **78**, 033835 (2008).

[14] J. Zeng, B.A. Malomed, *Phys. Rev. A* **85**, 023824 (2012).

[15] A. Rao, M. Malinowski, A. Honardoost, J.R. Talukder, P. Rabiei, P. Delfyett, S. Fathpour, *Opt. Express* **24**, 100066 (2016).

[16] S.T. Cundiff, B.C. Collings, N.N. Akhmediev, J.M. Soto-Crespo, K. Bergman, W.H. Knox, *Phys. Rev. Lett.* **82**, 3988 (1999).

[17] G.D. Shao, J. Guo, X. Hu, Y.F. Song, L.M. Zhao, D.Y. Tang, *Laser Phys. Lett.* **16**, 085110 (2019).

[18] X. Hu, J. Guo, G.D. Shao, Y.F. Song, S.W. Yoo, B.A. Malomed, D.Y. Tang, *Opt. Express* **27**, 18311 (2019).

[19] X.-W. Yan, J. Zhang, *Nonlinear Dyn.* **100**, 3733 (2020).

[20] F.H. Qi, B. Tian, X. Lü, R. Guo, Y.S. Xue, *Commun. Nonlinear Sci. Numer. Simul.* **17**, 2372 (2012).

[21] V.N. Serkin, T.L. Belyaeva, I.V. Alexandrov, G.M. Melchor, *Proc. SPIE* **4271**, 292 (2001).

[22] Z. Birnbaum, B.A. Malomed, *Physica D* **237**, 3252 (2008).

[23] S. Das, G.A. Sekh, *Fiber Integr. Opt.* **39**, 122 (2020).

[24] S. Das, K.K. Dey, G.A. Sekh, *Optik* **247**, 167865 (2021).

[25] R.M. Caplan, R. Carretero-González, P.G. Kevrekidis, B.A. Malomed, *Math. Comput. Simul.* **82**, 1150 (2012).

[26] C. Menyuk, *IEEE J. Qunatum Electron.* **23**, 174 (1987).

[27] R. Hao, L. Li, Z. Li, R. Yang, G.S. Zhou, *Opt. Commun.* **245**, 383 (2005).

[28] J.-R. He, L. Yi, H.-M. Li, *Phys. Rev. E* **90**, 013202 (2014).

[29] D. Anderson, *Phys. Rev. A* **27**, 3135 (1983).

[30] N.G. Vakhitov, A.A. Kolokolov, *Radiophys. Quantum Electron.* **16**, 783 (1973).

[31] D.E. Pelinovsky, Y.S. Kivshar, *Phys. Rev. E* **62**, 8668 (2000).

[32] B.A. Malomed, D.J. Kaup, R.A. Van Gorder, *Phys. Rev. E* **85**, 026604 (2012).

[33] G. Millot, P. Tchofo-Dinda, in: *Encyclopedia of Modern Optics*, 2005, p. 56.

[34] A. Mohamadou, C.G.L. Tiofack, T.C. Kofané, *Phys. Rev. E* **82**, 016601 (2010).

[35] G.P. Agrawal, *Applications of Nonlinear Fiber Optics*, Academic Press, 2001.

[36] Y.-F. Chen, K. Beckwitt, F.W. Wise, B.G. Aitken, J.S. Sanghera, I.D. Aggarwal, *J. Opt. Soc. Am. B* **23**, 347 (2006).